

Climate Policy Uncertainty and the Green Transition*

Sebastian Kreuzmair[†]

November 10, 2025
[Find the latest version here.](#)

Abstract

Carbon pricing is a key policy instrument to induce a green transition. However, political support for carbon pricing is uncertain and may change over time. I study the green transition in the electricity sector when climate policy switches stochastically between regimes with and without a carbon tax. I find that regime risk slows the transition: relative to a scenario with the tax implemented constantly, green electricity capacity builds up more slowly and brown capacity is invested in for longer, resulting in more carbon emissions during the transition. The rate at which the government switches regimes only has a limited effect on median outcomes at the end of the century. But longer expected durations lead to larger forecast intervals for the transition paths, with worse outcomes at the lower tail. This dispersion effect arises because infrequent switching makes any realized regime change more persistent, pushing the economy further from the deterministic-tax benchmark before averaging back. Thus, while frequent switching of government parties reduces the effective tax rate over the whole transition horizon, it also mitigates the risk of being stuck in a no-tax regime for a majority of the transition period.

JEL classification: O44, Q43, Q48, Q54, Q58

Keywords: climate policy uncertainty, green transition, investment

*I thank Florian Wagener, Jan Tuinstra, Andrea Titton, and Viola Vavrovsky for helpful comments and discussions.

[†]s.t.kreuzmair@uva.nl, University of Amsterdam & Tinbergen Institute

1 Introduction

Climate policy in many democracies is unstable, producing frequent reversals that shift the expected path of carbon prices and targets. In the United States, the Clean Power Plan (CPP) targeted a 32% reduction from 2005 emissions by 2030; it was replaced by the Affordable Clean Energy rule with much weaker expected impacts, including projections of under 1% reductions by 2030 relative to a baseline without the CPP (Shouse et al., 2020; U.S. EPA, 2015). Australia’s 2014 repeal of its electricity-sector carbon price and province-level pushback against Canada’s federal framework tell the same story. These episodes indicate policy paths that are hard to forecast and hence hard to invest against at long horizons. This empirical pattern motivates our analysis of how volatility in the future path of policy, not just its mean, maps into investment.

Policy uncertainty can depress investment where capital is durable and costly to adjust. The energy sector fits this profile and is central to mitigation: it is the largest source of greenhouse-gas emissions, and the transition requires large additions to clean capacity (IPCC, 2023). Power-generation and network assets are long-lived, difficult to repurpose, and adjust slowly because planning, permitting, and construction entail long lead times and other frictions. Given slow and costly adjustment, uncertainty about the policy path makes deferring non-urgent projects relatively more attractive, shifting investment toward later periods. Durability amplifies this effect because policy shocks affect returns over long horizons. This mechanism motivates our focus on energy and on how volatility in the policy path, not just its average level, shapes investment.

I model a representative electricity producer that chooses irreversible investment in green (renewable) and brown (fossil) capital under a carbon tax that switches between two political regimes. The government is formed by one of two parties: a green party that implements an exogenous carbon tax schedule and a brown party that does not implement any carbon tax. Government control follows a two-state Markov process with a constant hazard, so the firm faces uncertainty about the future tax path when planning capacity. Green capacity features learning-by-doing: as cumulative green capital rises, the unit cost of additional green capacity falls. At current demand, green is not yet cost-competitive with brown without a carbon tax, so the firm trades off near-term low-cost brown investment against building green capacity to unlock learning and to hedge against future taxes. This setup isolates how policy volatility interacts with learning to shape the timing and composition of investment during the transition.

The carbon-tax regime's stochastic switching slows the green transition relative to a deterministic benchmark in which the green-party tax is applied continuously with its full magnitude. Time spent in the no-tax regime lowers the effective carbon price faced by firms, delaying green investment and encouraging brown expansion. Because investment is irreversible, this brown expansion creates lock-in, so when the tax resumes the system cannot pivot quickly, lengthening the transition.

Changing the expected government duration alters persistence but not the long-run share of time in each regime. Thus, median transition paths are similar across switching rates. For short expected durations, frequent switching leads to realized transition paths that closely track the median. Longer expected durations widen forecast intervals because any regime switch then moves the economy farther from the median path, as the new regime is expected to last longer. This dynamic amplifies uncertainty around the transition.

Starting in a taxed regime with long expected durations leads to lowest cumulative emissions by century's end, even if median pollution levels are similar across durations. The high persistence of the initial taxed regime leads to earlier green investment and less brown expansion, resulting in lower emissions throughout the first half of the century. If a switch to no tax occurs later, brown investment rebounds and raises late-century emissions, leading to similar median pollution levels. The effect of lower early emissions dominates, however, so cumulative emissions fall as expected duration lengthens.

This paper builds upon the literature on investment under uncertainty and irreversibility (Abel, 1983; Dixit, 1992; Pindyck, 1991). If investment is irreversible, or comes with adjustment costs, firms may delay investment decisions in the face of uncertainty. Hassett and Metcalf (1999) analyze the effect of stochastic tax policy following a random walk or a stationary Poisson jump process on the time and size of investment in a single investment project. They find that increasing the variance of tax policy leads to earlier investment in case of a jump process, but to delayed investment in case of a random walk. The stationarity of the jump process implies that once a firm is in a good tax state there is little upside to further wait to invest. This does not directly apply to the present paper, as I consider continuous investment in two capital stocks with relative investment incentives changing depending on the tax state, such that the firm will generally want to invest in both states.

Two contributions in the field of climate-economics with irreversible investment closely related to the present paper are Rozenberg et al. (2020) and Baldwin et al. (2020). Rozenberg et al. (2020) analyze the effect of optimal carbon taxes on polluting asset

stranding in a single-sector economy with irreversible investment in capital. They find that the optimal carbon tax leads to premature retirement of polluting assets and analyze other policy instruments that can lead to the same long-term outcome but without stranding existing assets, which may be politically more feasible. Baldwin et al. (2020) focus on how learning-by-doing and irreversible investment affect the first-best optimal climate policy in a multi-sector economy with learning-by-doing in the green sector and irreversible investment in energy capital. They find that it is optimal to stop investing in brown technologies earlier than if investment were reversible and invest more in green technologies than if there were no learning-by-doing. In contrast to these two contributions, I do not solve for the first-best optimal climate policy, but analyze how uncertainty about the climate policy itself affects the energy sector's investment decisions in green and brown technologies and the duration of the green transition.

Aghion et al. (2016) and Calel and Dechezleprêtre (2016) show that carbon taxes can reallocate innovation toward clean technologies and away from polluting ones. While I do not consider endogenous technological change in this paper, the learning-by-doing in green technologies captures some aspects of directed technological change, as the carbon tax incentivizes investment in green technologies, which leads to cost reductions through learning effects. Acemoglu et al. (2012) model the process by which green and brown technologies evolve directly through R&D investments and show that the presence of a carbon tax can shift innovation towards green technologies.

The majority of the literature on optimal climate policy focuses on environmental and economic uncertainty, such as the uncertainty about the climate sensitivity to greenhouse gas emissions, the uncertainty about the costs of mitigation technologies, tipping points in the climate system, or other uncertainties about climate damages (see e.g. Cai, 2021, for an overview). In contrast, I assume full certainty about the climate and economic system, but uncertainty about the government's carbon tax policy. Fried et al. (2022) study how beliefs about the implementation of a new carbon tax, when there was none before, affect the investment decisions in green and brown technologies. They find that the implementation uncertainty leads to a steady state with lower emissions relative to a steady state without uncertainty through a combination of relatively cleaner investments and lower output. Their focus is on how pre-tax steady states differ under uncertainty about the carbon tax, while I focus on the dynamic effect of a continuously switching carbon tax regime on the transition to a steady state. Campiglio et al. (2024) analyze how firms with heterogeneous, adaptive beliefs about the actual implementation of future carbon taxes invest in green and brown technologies, and how this feeds back into the

government's decision to implement a carbon tax. They find low- and high-carbon equilibria coexisting, depending on the policy maker's credibility. In contrast to their focus on the feedback loop between firms' beliefs and government policy, I take the government's stochastic switching policy as given and analyze how this uncertainty affects the firm's investment decisions and the speed of the green transition under rational expectations.

Another approach to modeling less strict climate policy than a conventional social planner would implement is to analyze situations where the policy makers are dynamically inconsistent. Then policy makers cannot commit to a future policy path and future policy makers would like to deviate from the policy path chosen by the previous policy maker. This inconsistency may make the future climate policy less credible and the current climate policy less ambitious, which may lead to a delay in the green transition if not addressed. Time inconsistent policy makers can arise due to political competition, where a policy maker cannot guarantee that they will remain in power (Harstad, 2020) or due to political pressure from interest groups (Kalk & Sorger, 2023).

The remainder of this paper is structured as follows: In Section 2, I present the model and Section 3 discusses the calibration. In Section 4, I analyze the firm's investment decisions in green and brown technologies under the government's stochastic carbon tax policy. Section 5 discusses the implications of the results, and Section 6 concludes.

2 Model

In this section, I present the model which consists of a representative energy firm that invests in green and brown technologies and produces electricity using a constant elasticity of substitution (CES) production function, a political sector that stochastically switches between a regime with an exogenous carbon tax and a regime without a carbon tax, and an exogenous energy demand.

2.1 Political sector

The political system consists of two parties: one party is endowed with an exogenously given tax rule $\tau = \psi(P)$ of the form

$$\psi(P) = \tau_0 \left(e^{(\tau_1(P/P^P - 1))} - 1 \right), \quad (1)$$

where P is the atmospheric carbon concentration and P^P is the preindustrial carbon concentration. This functional form captures the idea that the social cost of carbon is an increasing and convex function of deviations of atmospheric carbon concentration from the preindustrial level. The specific form is chosen for analytical tractability and to allow for a calibration to existing carbon price scenarios, as discussed in Section 3. Note also that the climate dynamics in this model do not allow for carbon concentrations to fall below the preindustrial level, so the tax is always non-negative and zero when $P = P^P$.

The other party is endowed with a tax rule $\tau = 0$, meaning they do not implement a carbon tax. This captures a political scenario where one party actively seeks to implement climate policies while the other party opposes them and is able to reverse previous climate policy easily like the change of the Clean Power Plan (CPP) to the Affordable Clean Energy (ACE) rule in the US¹.

Mathematically, I describe the possibility of policy reversals by a stochastic regime-shift process that selects one of the two parties to form a government. Thus, the government can be in one of two states $m \in \{0, 1\}$. If $m = 0$, the brown party constitutes the government and the carbon tax is zero. If $m = 1$, the green party forms the government and implements a carbon tax according to $\psi(P)$. The government switches from one state to the other with a constant hazard rate λ . Thus, the political regimes follow a continuous-time Markov chain with two states, $m \in \mathcal{M} = \{0, 1\}$, where 1 denotes green government and 0 denotes brown government.

2.2 Energy sector

The energy sector is described by a representative firm that produces energy using green and brown capital stocks. The firm chooses investment in green and brown capital stocks I^G and I^B , as well as the utilization rates of green and brown energy $\eta = [\eta_G, \eta_B] \in [0, 1]^2$ to maximize profits. The utilization rates determine the fraction of installed capacity that is used to produce energy. A utilization rate of 0 means that the capital stock is not used at all, while a utilization rate of 1 means that the capital stock is used at full capacity.

¹This is naturally not the case for all climate policy and other interesting specifications would be to have a tax that is frozen in place, i.e., $\tau = \tau_{t_s}$ where t_s is the last time point the party implementing an active climate policy formed the government, or a tax that decreases at some rate, e.g. exponentially $\dot{\tau}_t = -\varpi\tau_t$, which could capture a party that is determined to reverse climate policy but is not able to do so immediately. I leave these alternative specifications for future research.

Energy is produced according to a CES production function

$$Z = F(\eta_G G, \eta_B B) = A^Z H(\eta_G G, \eta_B B) = A^Z (\xi (\eta_G G)^\gamma + (1 - \xi) (\eta_B B)^\gamma)^{\frac{1}{\gamma}}, \quad (2)$$

where A^Z is the total factor productivity of the energy sector, G and B are the green and brown capital stocks respectively, and η_G and η_B are the utilization rates of green and brown capital. The parameter ξ relates to the distribution of the relative factor shares in output and γ determines the elasticity of substitution between green and brown energy.

Capital is accumulated according to

$$\dot{G} = I^G - \delta_G G, \quad (3)$$

$$\dot{B} = I^B - \delta_B B, \quad (4)$$

where δ_K is the depreciation rate of capital $K \in \{G, B\}$.

The costs of investment, i.e., installation of new green and brown capital, consist of two parts: the costs of the investment itself and adjustment costs, which are a convex function of the investment size relative to the existing capital stock. I assume that brown energy technology has matured and therefore all cost parameters are constant. Total investment costs in brown energy are given by

$$\left(p^B + \frac{\kappa_B}{2} \frac{I^B}{B} \right) I^B, \quad (5)$$

where p^B is the price of new brown energy capital and κ_B is the adjustment cost parameter. The adjustment cost parameter κ determines how costly it is to increase capacity quickly.

The costs of investment in green energy are given by

$$\left(p^G(G) + \frac{\kappa_G}{2} \frac{I^G}{G} \right) I^G, \quad (6)$$

where $p^G(G)$ is the price of new green energy capital as a function of the installed green capital stock G , and κ_G is the adjustment cost parameter. The price of new green energy capital is given by

$$p^G(G) = p_0^G \left(\frac{G}{G_0} \right)^{-b}, \quad (7)$$

where p_0^G is the price of new green energy capital at the initial level of green capital G_0 and b determines the progress rate, i.e., the amount by which the price of green energy capital decreases if the energy capital stock is increased by a certain factor relative to the baseline. For example, doubling the green capital stock will lead to a price decrease of 2^{-b} . This specification of learning-by-doing is the same as in Baldwin et al. (2020), which is based on the literature on experience curves (Arrow, 1962; Wright, 1936).

Learning-by-doing at the aggregate level, i.e., depending on the aggregate installed green capital stock, will lead to an externality in a model with multiple firms, as individual firms do not take into account that their investment in green capital will lead to lower prices for all firms in the future. As I model a representative firm, this externality is not present in the current model. Having the learning-by-doing externality not be internalized would reduce the speed of the green transition further, as the individual firm would invest less in green energy capital. Thus, the duration of the green transition found in this model can be seen as a lower bound on the duration of the green transition in a more realistic setting with multiple firms.

The profit function is given by

$$\begin{aligned}\pi_m^Z(G, B, P) = & q(\eta_G G, \eta_B B) F(\eta_G G, \eta_B B) \\ & - \left(p^G(G) + \frac{\kappa_G}{2} \frac{I^G}{G} \right) I^G - \left(p^B + \frac{\kappa_B}{2} \frac{I^B}{B} \right) I^B \\ & - m\psi(P) \phi \eta_B B,\end{aligned}\tag{8}$$

where $q(\cdot)$ is the price of energy as determined by the demand function in Equation (16).

The energy firm maximizes the present discounted value of profits, i.e.

$$\max_{I^G \geq 0, I^B \geq 0, \eta \in [0, 1]^2} \mathbb{E} \left[\int_0^\infty e^{-\rho t} \pi_m^Z(\eta_G G, \eta_B B, P) dt \right],\tag{9}$$

subject to the accumulation equations for green and brown capital, and where ρ is the exogenous and constant discount rate. The expectations are taken over the stochastic process of the government's policy.

The solution to the problem is given by the value function $V_t(G, B, P, m)$, which is

determined by the Hamilton-Jacobi-Bellman (HJB) equation

$$\begin{aligned} \rho V_t(G, B, P, m) = & \max_{I^G \geq 0, I^B \geq 0, \eta \in [0, 1]^2} \{ q_t(F(\eta_G G, \eta_B B)) F(\eta_G G, \eta_B B) \\ & - \left(p^G(G) + \frac{\kappa_G}{2} \frac{I^G}{G} \right) I^G - \left(p^B + \frac{\kappa_B}{2} \frac{I^B}{B} \right) I^B - \psi(P, m) \phi \eta_B B \\ & + V_{t,G} \dot{G} + V_{t,B} \dot{B} + \dot{V}_t + \lambda (V_t(G, B, P, -m) - V_t(G, B, P, m)) \} , \end{aligned} \quad (10)$$

for $m \in \{0, 1\}$ and where $V_{t,G}$ and $V_{t,B}$ are the partial derivatives of the value function with respect to G and B at time t , respectively. If the firm fully internalized the pollution externality, it would include an additional drift term in the HJB equation $V_{m,P} \dot{P}$. However, the firm does not internalize the pollution externality, so I set $\dot{P} = 0$ in the HJB equation.

Optimal investments are determined by the FOCs

$$p^G + \kappa_G \frac{I^G}{G} = V_{t,G}, \quad (11)$$

$$p^B + \kappa_B \frac{I^B}{B} = V_{t,B}. \quad (12)$$

Optimal capital utilization rates $\eta = [\eta_G, \eta_B]$ satisfy the Karush-Kuhn-Tucker (KKT) conditions

$$\eta_K^* = \begin{cases} 0 & \text{if } \partial_{\eta_K} \pi^Z(0, \eta_{-K}^*) < 0 \\ \eta_K & \text{if } \partial_{\eta_K} \pi^Z(\eta_K, \eta_{-K}^*) = 0 \\ 1 & \text{if } \partial_{\eta_K} \pi^Z(1, \eta_{-K}^*) > 0 \end{cases} . \quad (13)$$

The elements of the gradient of the profit function with respect to the utilization rates are

$$\begin{aligned} \partial_{\eta_K} \pi^Z(\eta_G G, \eta_B B) = & \frac{\partial q}{\partial Z} F_K(\eta_G G, \eta_B B) F(\eta_G G, \eta_B B) K \\ & + q(F(\eta_G G, \eta_B B)) F_K(\eta_G G, \eta_B B) K \\ & - \mathbb{1}_{K=B} \psi(P, m) \phi K, \end{aligned}$$

where F_K is the marginal product of capital $K \in \{G, B\}$.

In case a tax is in place, this yields a system of two equations in two unknowns that can be solved numerically. If there is no tax in place, the two equations are identical and the system is underdetermined. In this case, I assume a tie-breaking rule that selects the utilization rate pair with the least amount of brown energy use. The exact optimality conditions for the utilization rates are given in Appendix A.

2.3 Environment

Using brown energy B generates emissions E . The emissions are given by

$$E = \phi \eta_B B, \quad (14)$$

where ϕ is the emissions intensity of brown capital. Pollution evolves according to

$$\dot{P} = E - \vartheta (P - P^P), \quad (15)$$

where ϑ is the decay rate of pollution and P^P is the preindustrial pollution level. Including the preindustrial pollution level guarantees that the pollution stock does not decay below the preindustrial level even if emissions are zero.

2.4 Energy Demand

Energy demand is represented by a semi-log inverse demand function for electricity

$$q_t(Z) = \alpha_t - \beta \log(Z). \quad (16)$$

I assume that the demand function shifts over time due to changes in technology, preferences, and economic growth, and model this by increasing α_t over time, i.e.

$$\alpha_t = \alpha_0 \prod_{i=1}^t (1 + g_{\alpha,i}), \quad (17)$$

where $g_{\alpha,t}$ is the growth rate of α from time t to $t+1$. I assume β fixed to keep the semi-elasticity of demand constant over time to keep the model parsimonious and because there is little evidence on how the semi-elasticity of energy demand will change in the future.

3 Calibration

3.1 Political sector

I calibrate the tax rule $\tau = \psi(P)$ of the green party to different scenarios of Phase V (Richters et al., 2024) of the Network for Greening the Financial System (NGFS) based on the Remind-MAgPIE model (Baumstark et al., 2021; Dietrich et al., 2019). The scenarios provide carbon prices from 2020 to 2100 under different climate policy assumptions. They also include corresponding emission pathways, but no publicly

available carbon concentration data. To obtain estimated carbon concentrations, I use the simplifying assumption that emissions add directly to atmospheric carbon concentrations without any natural sinks. This is a simplification as the Remind-MAgPIE model includes the MAGICC climate module (Meinshausen et al., 2011), but given the focus of this paper on investment under political uncertainty, I abstract from a more detailed calibration of the climate module. These two components allow me estimate the parameters $[\tau_0, \tau_1]$ and calibrate the carbon price function $\psi(P)$ as a function of atmospheric carbon concentration P . Figure 1 shows the

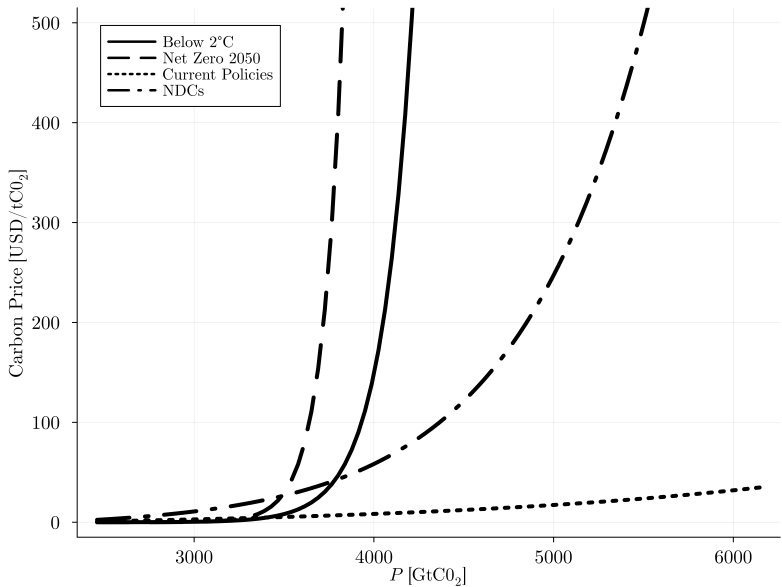


Figure 1: Carbon price function calibrated to NGFS Phase V scenarios.

calibrated carbon price functions for selected NGFS scenarios. The difference between the *Current Policies* scenario and the *Nationally Determined Contributions (NDCs)* scenario is that the *Current Policies* scenario only considers policies that are already implemented, while the *NDCs* scenario also considers announced policies that are not yet implemented. The other scenarios consider more ambitious climate policies and lead to higher carbon prices.

3.2 Energy sector

Figure 2 shows the level curves of the calibrated production function. To prevent the status-quo of the energy mix from determining the long-run outcome, I set the

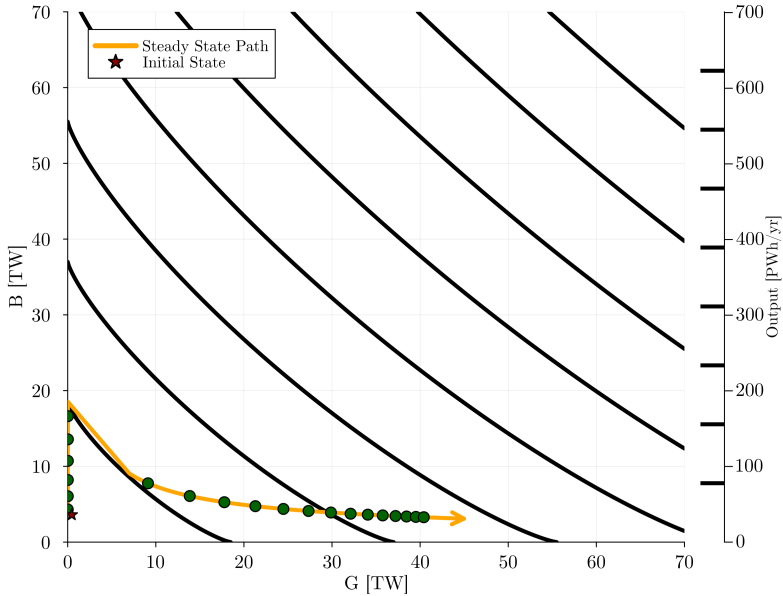


Figure 2: Optimal capital split between green and brown capital at time $t \in [2012, 2022, \dots, 2212]$ assuming that each point in time is a steady state and persists forever.

share parameter $\xi = 0.5$ in the baseline calibration. To allow for a meaningful green transition, I assume that green and brown energy are fairly substitutable with respect to each other with $\gamma = 0.8$, which implies an elasticity of substitution of $\sigma = \frac{1}{1-\gamma} = 5$.

Also depicted in Figure 2 are optimal capital stock splits between green and brown capital that correspond to demand levels along the calibrated demand path (see below), assuming that demand at each point in time persists forever and there is no carbon price. More precisely, I compute the optimal capital stock split by solving the static profit maximization problem

$$\max_{G \geq 0, B \geq 0} q_t(F(G, B)) F(G, B) \quad (18)$$

$$- \left(p^G(G) + \frac{\kappa_G}{2} \delta_G \right) \delta_G G - \left(p^B + \frac{\kappa_B}{2} \delta_B \right) \delta_B B, \quad (19)$$

where the firm chooses the steady-state level of green and brown capital to maximize profits given the demand function at time t .

The figure shows that to satisfy the initial rise in electricity demand, the firm would optimally invest in brown capital, as at that scale of production green capital is not yet

cost-competitive. However, as demand continues to rise and thus the required capital stock increases, green capital becomes more cost-competitive due to learning-by-doing and the firm would optimally start switching its capital stock to green capital. The irreversibility of investment and the presence of adjustment costs constitute a channel that could lead to a lock-in of brown capital, since a firm with a sufficiently high discount rate may be reluctant to invest in green capital early on when it is still more expensive than brown capital.

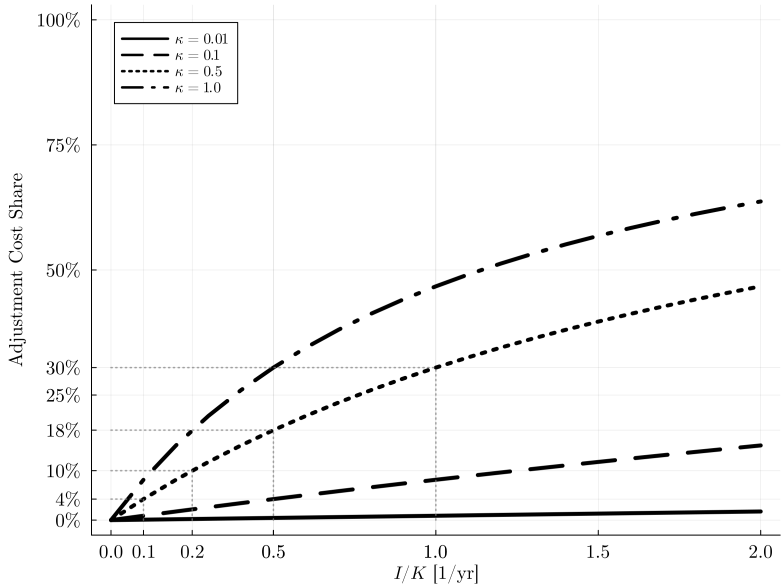


Figure 3: Share of adjustment costs in total investment costs as a function of the investment rate I/K in brown capital for different levels of κ .

Figure 3 shows how the share of adjustment costs in total investment costs increases with the investment rate I/K for different levels of κ . For example, if $\kappa = 0.5$, then doubling the existing capital stock leads to adjustment costs that are around 30% of total investment costs. For lower values of κ , adjustment costs are relatively small even for high investment rates. I set $\kappa_G = \kappa_B = 0.5$ in the baseline calibration to capture moderate adjustment costs.

Figure 4 shows the costs of replacing depreciated capital, i.e., $\left(p^K(K)\delta_K + \frac{\kappa_K}{2}\delta_K^2\right)K$ for $K \in \{G, B\}$, as a function of the capital stock. The costs of replacing depreciated brown capital are linearly increasing in the brown capital stock, while the costs of replacing depreciated green capital are decreasing in the green capital stock due to

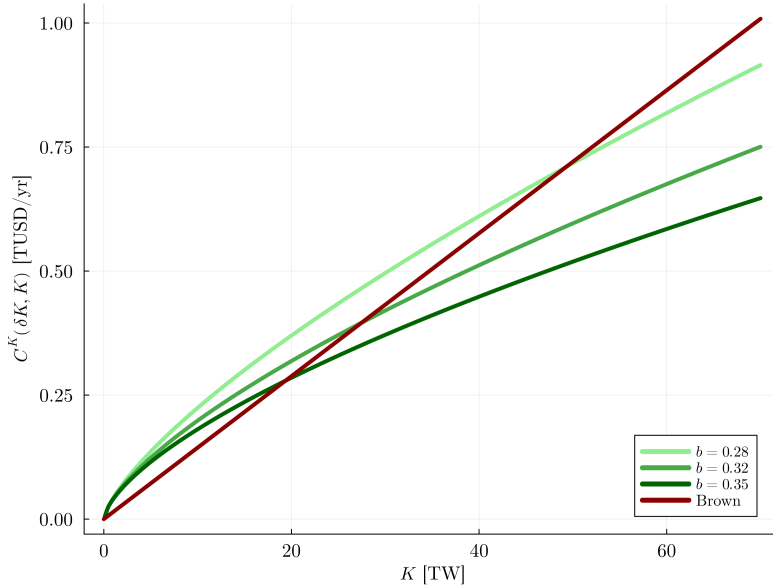


Figure 4: Costs of replacing depreciated capital as a function of the capital stock.

learning-by-doing. The figure shows that for low levels of green capital, replacement investment costs are higher than those of brown capital, but as the green capital stock increases, replacement investment costs become lower than those of brown capital. The cross-over point is influenced by the parameters of the investment cost function, in particular the learning rate b and the depreciation rates of capital δ_G and δ_B . I depart here from the calibration of Baldwin et al. (2020), as for the values of b and δ_G used in that paper, replacement investment costs for green capital in my model would always be higher than those of brown capital. As this does not align with observed trends in renewable energy costs, I adjust these parameters to ensure that replacement investment costs for green capital can become lower than those of brown capital at higher levels of the green capital stock. In my baseline calibration, I set² the learning rate $b = 0.32$ and depreciation rates $\delta_G = \delta_B = 0.025$. These depreciation rates correspond to an average lifespan of 40 years for both green and brown capital, which overstates the lifespan of current renewable energy capital. Together with the higher learning rate, this leads to replacement investment costs for green capital becoming lower than those of brown capital at around 25 TW of green energy capacity. The initial green capital stock is set to 0.46 TW, which includes all renewable energy sources except hydro power (see Appendix 3 for details).

²Compared to $b = 0.285$ and $\delta_G = 0.04$ and $\delta_B = 0.025$ in Baldwin et al. (2020).

3.3 Electricity Demand

The parameters α_t and β are calibrated such that the observed output Z_0 at time $t = 0$, which corresponds to the year 2012, is revenue-maximizing at q_0 , i.e., $\alpha_0 = \beta_0(1 + \log(Z_0))$ and $\beta = \beta_0 = q_0$.

The growth rates of α_t are calibrated to match projections of future electricity demand from the International Energy Agency and the IPCC. Specifically, I set the growth rates such that electricity demand (defined as the steady-state profit-maximizing output as described before) grows to around 55 PW h yr^{-1} in 2050 and 120 PW h yr^{-1} in 2100, which matches predictions from the *Stated Policies* scenario of the International Energy Agency for 2050 (International Energy Agency, 2024, see Figure 3.21) and the IPCC AR6 scenario ensemble median for both 2050 and 2100 (IPCC, 2023, see Figure 3.23).

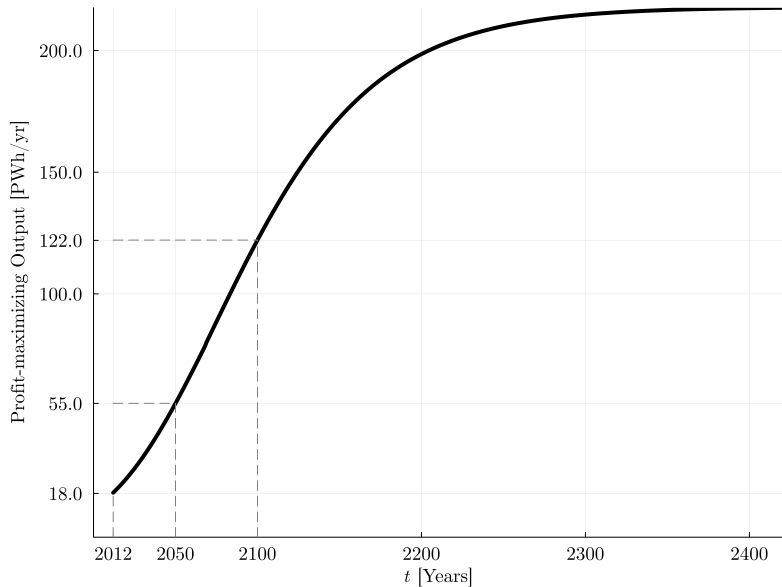


Figure 5: Profit-maximizing, steady-state output Z_t over time along the calibrated demand path.

Figure 5 shows the profit-maximizing output over time resulting from the calibrated demand functions.

3.4 Numerical Implementation

I solve the firm's optimal control problem using a semi-implicit finite difference upwind scheme (see e.g. Achdou et al., 2022; Candler, 1999). For details, see Appendix B.

4 Numerical Results

In this section, I present the numerical results of the model. I contrast the outcomes under two different policy scenarios: *Current Policies*, which only considers already existing policies, and *Nationally Determined Contributions (NDCs)* which also includes pledged but not yet implemented policies. As a robustness check, I also consider a third, more ambitious tax schedule in Section D.

I consider two benchmarks for each policy scenario. First, a deterministic benchmark in which the carbon tax is implemented permanently at the levels specified by the respective policy scenario, the deterministic full-tax case. Second, a deterministic benchmark with the carbon tax at the average level between the two regimes, the deterministic average-tax case. Given that in the no-tax regime the carbon price is zero, this average tax is simply half the tax level in the full-tax regime.

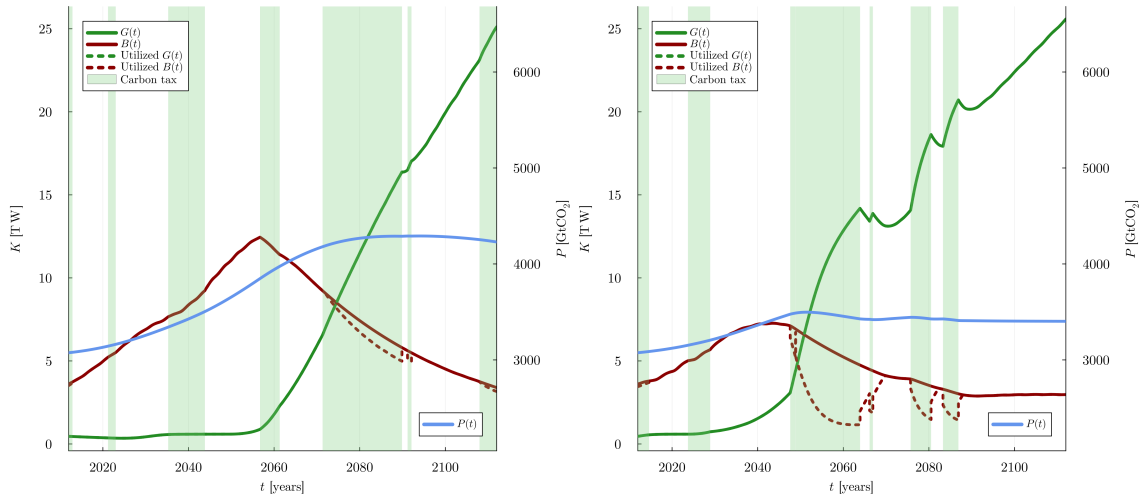


Figure 6: Evolution of state variables under *Current Policies* (left column) and *NDCs* (right column) with an expected government duration of 8 years.

Figure 6 shows the evolution of the state variables under the *Current Policies* and the *NDCs* scenario with an expected government duration of 8 years. This duration

is consistent with the two-term limit for elected officials in many jurisdictions. It also leads to a reasonable number of regime switches, while still allowing regimes with some stability, which illustrates the mechanism well. The carbon price in the *Current Policies* scenario is low and increases slowly over time. Combined with the uncertainty about the actual implementation, this results in an initial expansion of brown energy capacity. From around 2060 onwards, a combination of rising carbon prices and increased electricity demand leads to a shift from brown to green energy. The speed of this transition is higher in periods with a tax in place (albeit only slightly). The irreversibility of investment decisions leads to a lock-in of brown capacity, which only starts to decline significantly once the carbon tax reaches higher levels later in the century. But the carbon tax is not high enough to deter the firm from fully utilizing its brown capacity, and only speeds up green investment slightly.

The right column of Figure 6 displays the results under the *NDCs* policy scenario, again with an expected government duration of 8 years. In this case, the carbon tax starts at a higher level and increases more rapidly over time. This leads to an immediate increase in green energy capacity and a smaller expansion of brown capacity compared to the *Current Policies* scenario. The higher carbon tax also leads to underutilization of brown capacity in taxed periods, in combination with increased green investment. Switching to the no-tax regime results in a temporary rebound in brown energy utilization and investment, but only slows down the overall transition to green energy, not reversing it.

Figures 7, 8, and 9 provide a direct comparison of brown energy capacity, green energy capacity, and pollution levels under the two policy scenarios for different expected government durations.

Contrasting the two scenarios, it is evident that the magnitude of the carbon tax significantly affects the investment decisions of the energy firm. The *NDCs* scenario leads to earlier and more substantial investments in green energy capacity, as well as a faster reduction in brown energy capacity. This results in lower pollution levels throughout the entire simulation horizon compared to the *Current Policies* scenario, regardless of the expected government duration.

With longer expected regime durations, the early transition tracks the deterministic path that holds the initial regime fixed, because a switch is unlikely over that horizon. This persistence does not create self-sustaining momentum: when a later switch to a no-tax regime occurs, brown investment resumes and the transition slows. Hence, within each policy scenario, medians at the end of the century change little across durations; what duration mainly shifts is the spread around those medians.

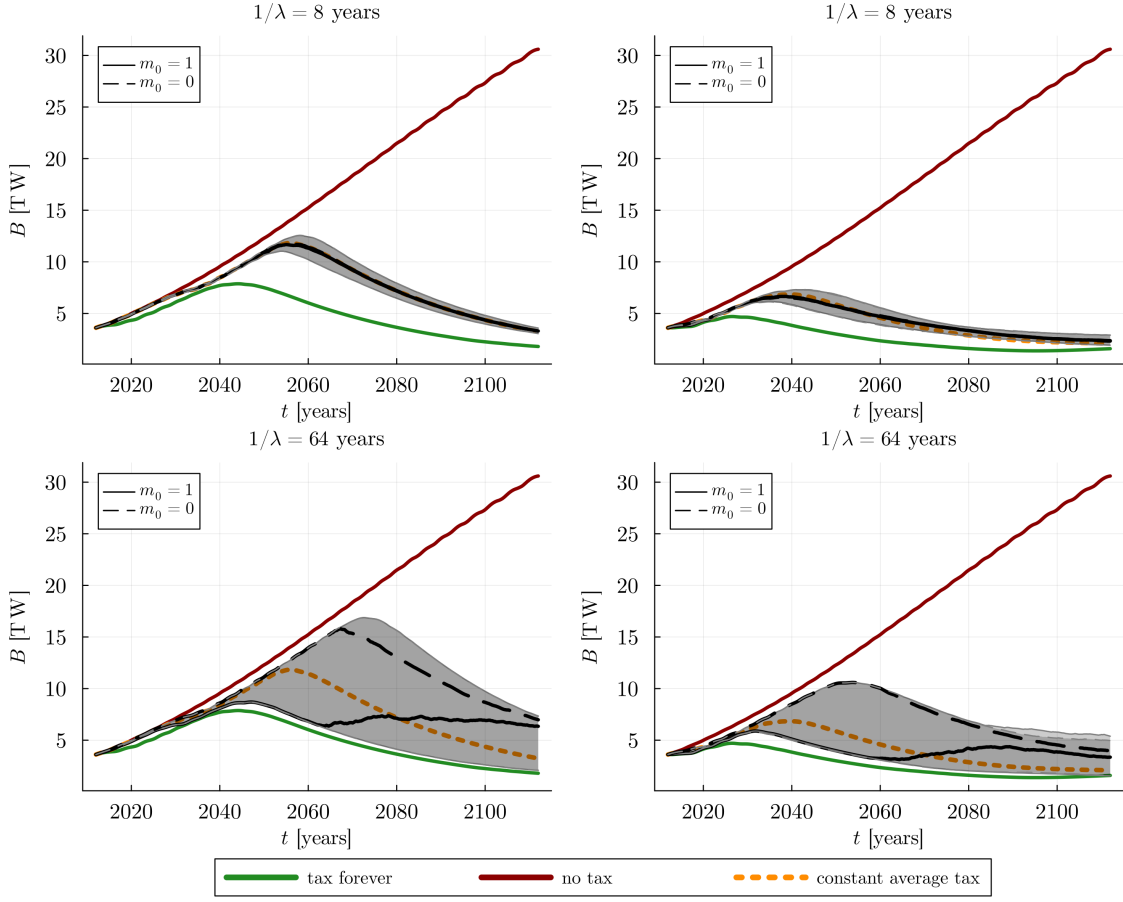


Figure 7: Comparison of brown energy capacity under *Current Policies* (left column) and *NDCs* (right column) including the median and the 10th and 90th percentiles of brown energy capacity over time.

The uncertain policy duration reduces the speed of transition in both scenarios compared to a setting with the full carbon tax permanently implemented. The difference is economically significant: adding policy uncertainty increases the median pollution level in 2112 by approximately 590 Gt CO₂ in the *Current Policies* scenario compared to a deterministic full tax implementation. In the *NDCs* scenario, this increase is reduced to approximately 240 Gt CO₂.

Relating this to the global carbon budget of 1150 Gt CO₂ for a 67% chance of limiting warming to 2 °C (IPCC, 2021), this increase in pollution levels corresponds to an additional 857 Gt CO₂ and 455 Gt CO₂ emitted by 2112 due to policy uncertainty in

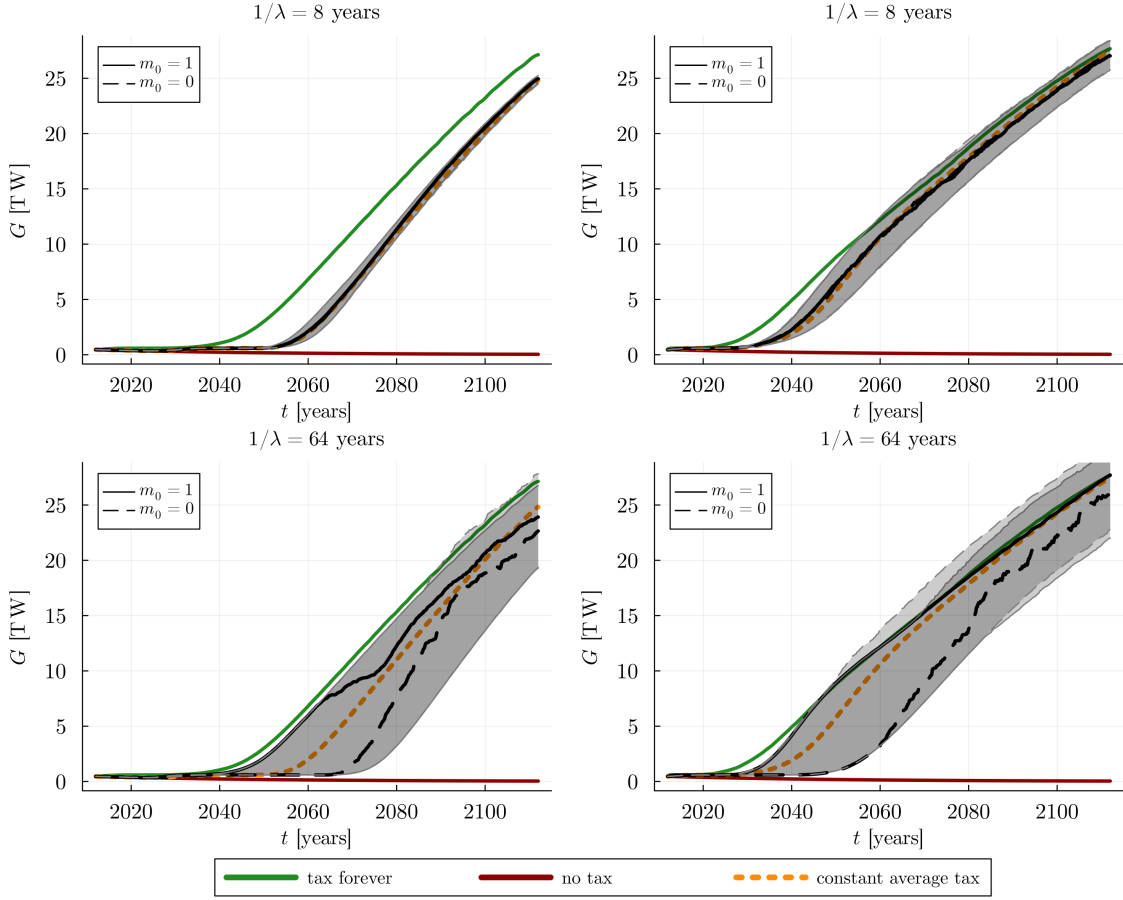


Figure 8: Comparison of green energy capacity under *Current Policies* (left column) and *NDCs* (right column) including the median and the 10th and 90th percentiles of green energy capacity over time.

the *Current Policies* scenario, and 417 Gt CO₂ and 121 Gt CO₂ in the *NDCs* scenario, for expected government durations of 8 years and 64 years, respectively.

Figure 10 shows the difference in cumulative emissions relative to the deterministic full-tax benchmark under both policy scenarios for different expected government durations. In both scenarios, cumulative emissions exhibit relatively constant levels for expected government durations up to 16 years. However, for longer expected durations, cumulative emissions begin to decrease. They exhibit a sharp decline between expected durations of 32 and 64 years, as the longer persistence of the initial tax regime leads to more substantial reductions in emissions early in the century.

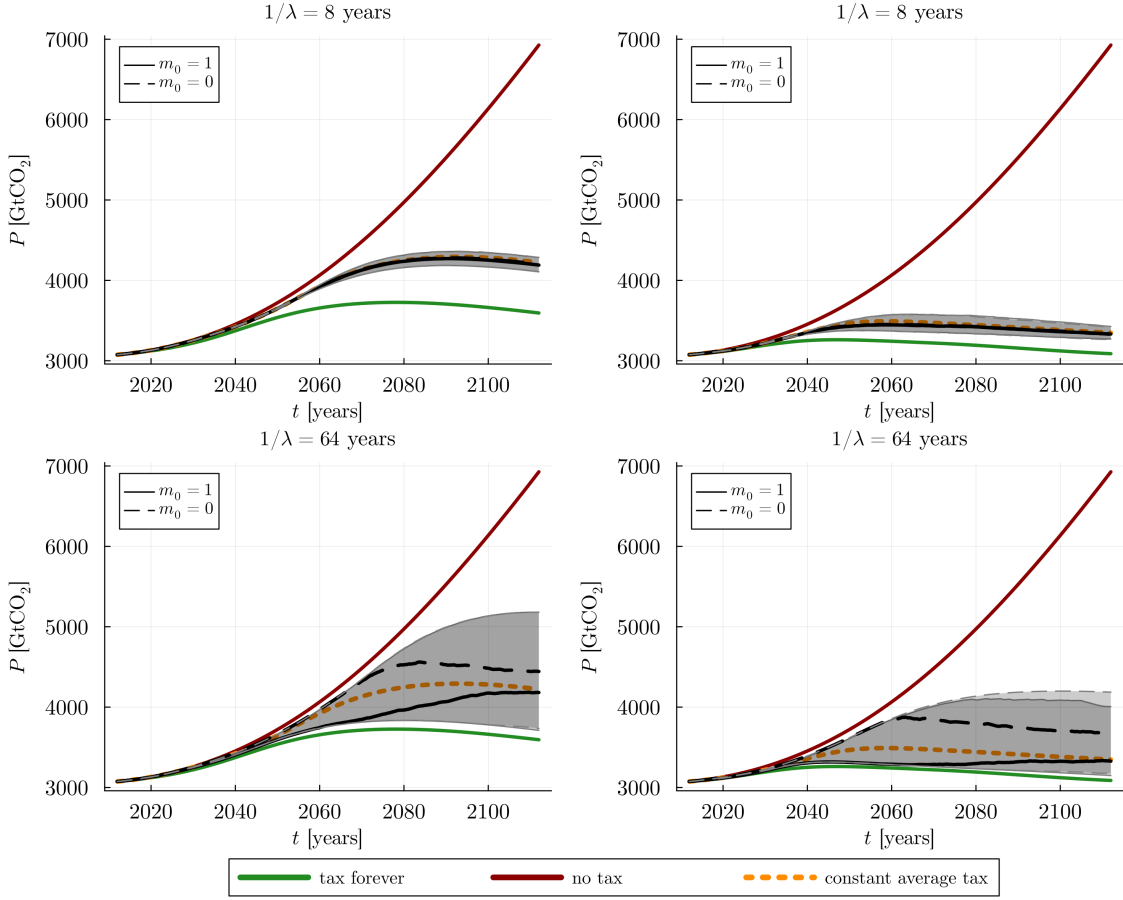


Figure 9: Comparison of pollution levels under *Current Policies* (left column) and *NDCs* (right column) including the median and the 10th and 90th percentiles of pollution levels over time.

The higher pollution stock in 2112 under longer expected regime durations arises because the likelihood of ending the horizon in a prolonged no-tax spell is higher, so emissions late in the century are higher and decay less.

There are two effects of policy uncertainty on cumulative emissions. The symmetric hazard rates mean that the long-run time share in taxed versus no-tax regimes is unchanged by changing expected durations. What differs is how this time is distributed over time and in particular across the shorter horizon of the transition. Short expected durations lead to frequent switching, which approximates a deterministic setting with an effective tax equal to half the statutory level. Thus, there are steady, but

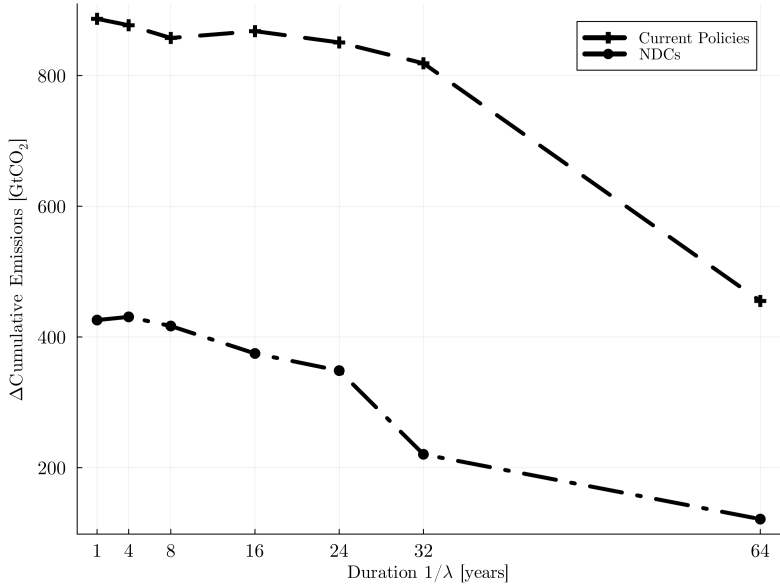


Figure 10: Difference in cumulative emissions relative to the deterministic full-tax benchmark under *Current Policies* and *NDCs* for different expected government durations.

reduced, incentives for green investment throughout the century. Whether this steady but lower tax suffices to shift the energy mix depends on the statutory level: under *Current Policies*, green investment starts much later (around 20 years) than under *NDCs* for short durations. For longer expected durations, the initial regime dominates early decades and provides stronger incentives if it is the tax regime. However, if a switch to the no-tax regime occurs, this is also expected to persist, leading to a potential rebound in brown investment and emissions later in the century that can offset early gains.

Policy uncertainty can also lead to overinvestment in green capacity relative to the deterministic benchmark. Policy uncertainty increases the time during which the firm expands brown capacity compared to the deterministic full-tax case, leading to higher pollution levels. This raises the carbon price in taxed regimes. Once the tax is in place, the firm then has stronger incentives to build green capacity as it will underutilize brown capacity during taxed periods to save on tax payments. This increases incentives to invest in green capacity to meet demand during taxed periods, leading to overinvestment relative to the deterministic benchmark. The effect of overinvestment is more pronounced under the *NDCs* scenario with its higher statutory

tax levels and with longer expected durations, where the firm may deviate more from the deterministic average tax path, because of the more persistent differences in investment incentives across regimes.

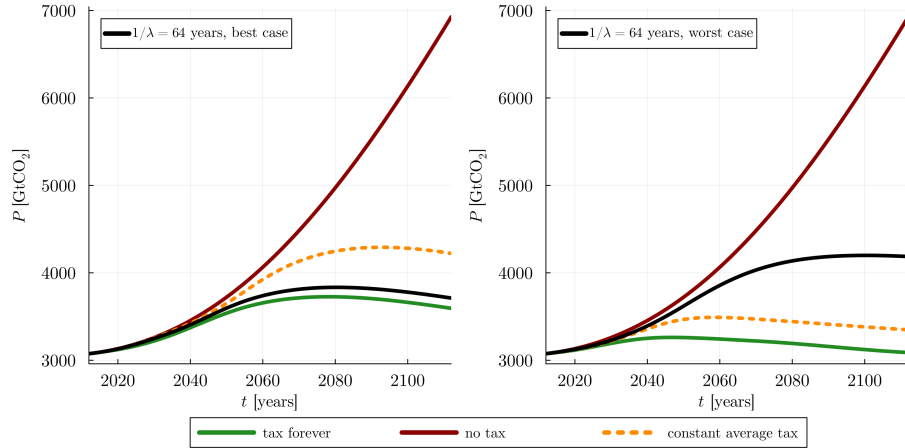


Figure 11: Pollution levels comparing the best-case scenario under *Current Policies* (left column, regime never switches to no tax) and the worst-case scenario under *NDCs* (right column, regime never switches to tax) with an expected government duration of 64 years.

A credible threat of higher future carbon tax can be more effective than a low but certain tax today even if the threatened tax is never implemented³. Figure 11 illustrates this by comparing the best-case scenario under *Current Policies*, where the firm expects a switch on average every 64 years but the regime never switches to no tax, to the worst-case scenario under *NDCs*, where the firm expects a switch on average every 64 years but the regime never switches to tax. Even in this extreme comparison, pollution levels under *NDCs* are comparable to the average tax benchmark under *Current Policies* and only rise moderately above the best-case *Current Policies* scenario.

The results discussed in this section so far hinge on the assumption that the initial regime is the tax regime. If the initial regime were the no-tax regime, the results would be similar for the shorter expected government durations, where the first regime switch is likely to happen early on, as can be seen in the dashed lines in Figures 7, 8, and 9. For longer expected government durations, the initial no-tax regime would be

³This of course assumes that the lack of implementation does not undermine the credibility of the threat.

likely to last for a significant portion of the transition horizon, leading to continued brown investment and delayed green investment. This results in higher pollution levels throughout the entire simulation horizon and much larger cumulative emissions.

Figures 12, 13, and 14 further analyze the interaction between expected government durations and carbon tax rates by showing the values of the state variables in 2112 across different combinations of these two parameters. The parameter τ_0 is held constant at levels corresponding to the *Current Policies* and *NDCs* scenarios, while τ_1 is varied to assess its impact on the transition outcomes.

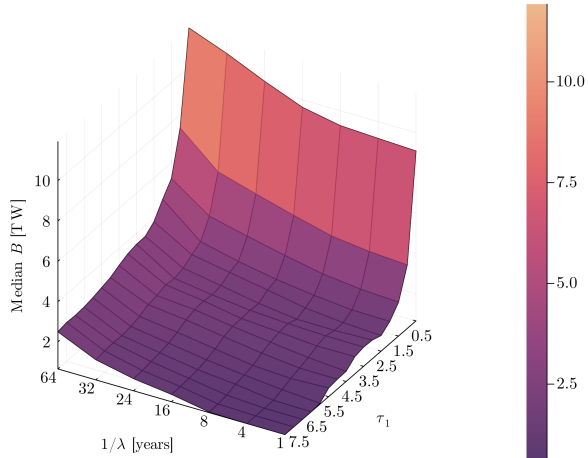


Figure 12: Brown energy capacity in 2112 across different expected government durations and tax rates.

Figure 12 shows that high carbon taxes coupled with short expected government durations lead to the lowest brown energy capacity in 2112. This is because frequent switching between regimes results in an averaged tax rate that still provides significant incentives for phasing out brown energy, but does not run the risk of being stuck in a no-tax regime for extended periods. Conversely, low carbon taxes and long expected government durations result in the highest brown energy capacity, as the firm faces prolonged periods without sufficient incentives to reduce brown energy investments. High tax rates with long expected government durations also lead to higher brown capacity compared to short expected durations, as switching to a no tax regime may partially reverse earlier investments. Similarly, low tax rates with short expected government durations lead to lower brown capacity compared to long

expected durations, as the frequent switching provides more consistent incentives for reducing brown investments.

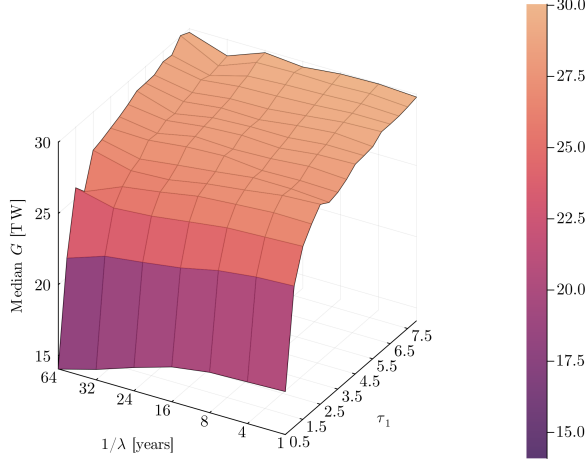


Figure 13: Green energy capacity in 2112 across different expected government durations and tax rates.

In Figure 13, it can be observed that higher carbon tax rates lead to increased green energy capacity in 2112, regardless of the expected government duration. The inverse effect for green capacity, of longer expected government durations leading to lower green capacity, is not present. This is because once green capacity is built up, it is not reduced even if the regime switches to no tax, but maintained anticipating future tax periods.

As shown in Figure 14, this results in lowest pollution levels in 2112 for combinations of high carbon tax rates and short expected government durations. Pollution levels are slightly rising with longer expected government durations for a given tax rate, but the effect is relatively small compared to the impact of the tax rate itself.

5 Discussion

The model implies that stochastic policy reversals slow the green transition relative to a deterministic carbon price path with otherwise identical fundamentals. Because time spent in the no-tax regime lowers the effective carbon price along the transition, the firm expands brown capacity more and builds green capacity more slowly; with

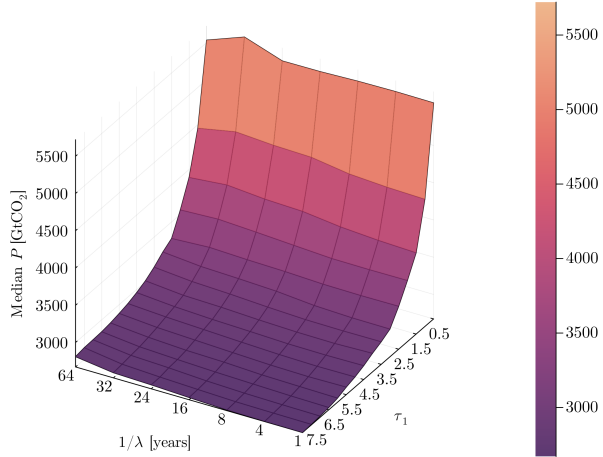


Figure 14: Pollution levels in 2112 across different expected government durations and tax rates.

irreversible investment, the inherited brown stock then prolongs adjustment once the tax returns.

The speed of government turnover shapes the dispersion of outcomes more than the center. Across policy schedules, changing the expected regime duration leaves median end-of-century outcomes similar but widens forecast intervals for capacities and emissions when expected durations are long. Longer expected durations increase the chance that any realized spell persists, so a switch—when it occurs—moves the economy farther from the median path; very fast switching instead makes the environment resemble a deterministic setting with an averaged tax. These forces lead to similar median pollution levels at the end of the century across expected durations. However, cumulative emissions are decreasing in expected duration as the longer time under tax in the early part of the century outweighs the rebound in brown investment if a no-tax spell occurs later on.

The magnitude of the tax level dominates expected durations for transition speed and pollution. Under the *NDCs* schedule, green capacity rises earlier and brown capacity falls faster than under *Current Policies* for any given expected duration, producing lower pollution over the whole horizon. Quantitatively, introducing policy uncertainty increases median 2112 pollution by about 590 Gt CO₂ under *Current Policies* but by only 240 Gt CO₂ under *NDCs*; even extreme comparisons—best-case *Current Policies* vs. worst-case *NDCs* with 64-year durations—show *NDCs* outcomes

that are competitive for most of the century. These patterns indicate that raising the carbon price has a larger effect than altering expected government duration.

Taken together, the results suggest two policy lessons. First, designs that keep the effective carbon price high—via higher statutory levels or credible future price paths—accelerate decarbonization more than changes in expected political durations. Second, when high statutory prices are infeasible, a credible threat of a high tax schedule being implemented in the future can outperform a low certain tax schedule today.

Scope and extensions. Four modeling choices bound external validity and motivate next steps. (i) *Binary reversals*. Regime changes are modeled as tax vs. no tax. Allowing partial persistence (e.g., freezing the tax at the last level) or gradual decay would raise the effective average price and likely attenuate, but not overturn, the main results by reducing carbon-price volatility. (ii) *Sector aggregation*. Treating the power sector as a single representative firm abstracts from interactions between fossil and renewable producers; splitting sectors and allowing market-share dynamics could amplify asymmetries when expected durations are long. (iii) *Exogenous politics*. Both the tax path within the green regime and the hazard of losing agenda control are exogenous. Endogenizing them through an explicit household sector with voting over taxes and climate damages would allow feedback from economic and environmental states to political durability. (iv) *Partial equilibrium*. Embedding the firm problem in a general equilibrium with multiple sectors and endogenous energy demand could adjust magnitudes via income and substitution effects and intertemporal pricing while preserving the qualitative rankings documented above.

6 Conclusion

I study investment under climate policy uncertainty in a continuous-time, two-regime model in which governments alternate between a zero-tax and a positive-tax regime. Relative to a deterministic benchmark that applies the positive tax continuously at its full magnitude, the possibility of switching lowers the effective carbon price. With irreversible capital, firms defer green investment and expand brown capacity; when the tax returns, the inherited brown stock slows adjustment and lengthens the transition. Across scenarios, the carbon-price level shifts outcomes more than expected regime duration.

The switching speed governs dispersion more than central tendency. With symmetric

hazards, changing the hazard λ alters persistence but not the long-run time share in each regime, so median paths move little. Longer expected durations widen forecast intervals because realized switches tend to persist and push capacity further before averaging back; as $\lambda \rightarrow \infty$, frequent flips average the policy path toward a deterministic effective price and forecasts tighten.

Cumulative emissions need not be monotone in expected duration. Two forces interact. Short expected durations compress the process toward an average price; if that average price is low, green investment lags and cumulative emissions are high, while a higher average price sustains steady green buildout. Long expected durations make the initial regime dominate early on; if a later switch moves to no tax, brown investment rebounds and raises late-century emissions, potentially offsetting early gains.

Policy design should therefore prioritize credible levels and durability: a binding floor under the carbon price, automatic escalation rules tied to concentrations or dates, and instruments that survive changes in government. These compress policy vacuums and tail risk, reducing delays in the transition. Two caveats remain. The analysis is partial equilibrium with exogenous within-regime tax paths, and the carbon cycle is deliberately simple. Extending the framework to general equilibrium and endogenous politics is a natural next step. The central message is unchanged: credibility and the carbon-price level determine the pace of the transition; expected regime duration mainly widens or narrows its uncertainty.

References

- Abel, A. B. (1983). Optimal Investment Under Uncertainty. *The American Economic Review*, 73(1), 228–233. Retrieved November 27, 2023, from <https://www.jstor.org/stable/1803942> (cit. on p. 3).
- Acemoglu, D., Aghion, P., Bursztyn, L., & Hemous, D. (2012). The Environment and Directed Technical Change. *American Economic Review*, 102(1), 131–166. <https://doi.org/10.1257/aer.102.1.131> (cit. on p. 4).
- Achdou, Y., Han, J., Lasry, J.-M., Lions, P.-L., & Moll, B. (2022). Income and Wealth Distribution in Macroeconomics: A Continuous-Time Approach. *The Review of Economic Studies*, 89(1), 45–86. <https://doi.org/10.1093/restud/rdab002> (cit. on pp. 16, 34).
- Aghion, P., Dechezleprêtre, A., Hémous, D., Martin, R., & Van Reenen, J. (2016). Carbon Taxes, Path Dependency, and Directed Technical Change: Evidence from the Auto Industry. *Journal of Political Economy*, 124(1), 1–51. Retrieved October 9, 2025, from <https://www.jstor.org/stable/26549857> (cit. on p. 4).
- Arrow, K. J. (1962). The Economic Implications of Learning by Doing. *The Review of Economic Studies*, 29(3), 155–173. <https://doi.org/10.2307/2295952> (cit. on p. 8).
- Baldwin, E., Cai, Y., & Kuralbayeva, K. (2020). To build or not to build? Capital stocks and climate policy. *Journal of Environmental Economics and Management*, 100, 102235. <https://doi.org/10.1016/j.jeem.2019.05.001> (cit. on pp. 3, 4, 8, 14, 37, 38).
- Barrage, L., & Nordhaus, W. (2024). Policies, projections, and the social cost of carbon: Results from the DICE-2023 model. *Proceedings of the National Academy of Sciences*, 121(13), e2312030121. <https://doi.org/10.1073/pnas.2312030121> (cit. on p. 37).
- Baumstark, L., Bauer, N., Benke, F., Bertram, C., Bi, S., Gong, C. C., Dietrich, J. P., Dirnachner, A., Giannousakis, A., Hilaire, J., Klein, D., Koch, J., Leimbach, M., Levesque, A., Madeddu, S., Malik, A., Merfort, A., Merfort, L., Odenweller, A., ... Luderer, G. (2021). REMIND2.1: Transformation and innovation dynamics of the energy-economic system within climate and sustainability limits. *Geoscientific Model Development*, 14(10), 6571–6603. <https://doi.org/10.5194/gmd-14-6571-2021> (cit. on p. 10).
- Cai, Y. (2021, February 23). The Role of Uncertainty in Controlling Climate Change. In *Oxford Research Encyclopedia of Economics and Finance*. <https://doi.org/10.1093/acrefore/9780190625979.013.573> (cit. on p. 4).
- Calel, R., & Dechezleprêtre, A. (2016). Environmental Policy and Directed Technological Change: Evidence from the European Carbon Market. *Review of Economics*

- and Statistics*, 98(1), 173–191. https://doi.org/10.1162/REST_a_00470 (cit. on p. 4).
- Campiglio, E., Lamperti, F., & Terranova, R. (2024). Believe me when I say green! Heterogeneous expectations and climate policy uncertainty. *Journal of Economic Dynamics and Control*, 165, 104900. <https://doi.org/10.1016/j.jedc.2024.104900> (cit. on p. 4).
- Candler, G. V. (1999). Finite-Difference Methods for Dynamic Programming Problems. In *Computational Methods for the Study of Dynamic Economies*. Cambridge University Press. (Cit. on p. 16).
- Dietrich, J. P., Bodirsky, B. L., Humpenöder, F., Weindl, I., Stevanović, M., Karstens, K., Kreidenweis, U., Wang, X., Mishra, A., Klein, D., Ambrósio, G., Araujo, E., Yalew, A. W., Baumstark, L., Wirth, S., Giannousakis, A., Beier, F., Chen, D. M.-C., Lotze-Campen, H., & Popp, A. (2019). MAgPIE 4 – a modular open-source framework for modeling global land systems. *Geoscientific Model Development*, 12(4), 1299–1317. <https://doi.org/10.5194/gmd-12-1299-2019> (cit. on p. 10).
- Dixit, A. (1992). Investment and Hysteresis. *The Journal of Economic Perspectives*, 6(1), 107–132. Retrieved March 25, 2024, from <https://www.jstor.org/stable/2138376> (cit. on p. 3).
- The Earth's Energy Budget, Climate Feedbacks and Climate Sensitivity. (2023). In IPCC (Ed.), *Climate Change 2021 – The Physical Science Basis: Working Group I Contribution to the Sixth Assessment Report of the Intergovernmental Panel on Climate Change* (pp. 923–1054). Cambridge University Press. <https://doi.org/10.1017/9781009157896.009> (cit. on p. 37).
- EIA. (2023, December). *Electric Power Annual 2012*. U.S. Energy Information Administration. Washington, DC. (Cit. on p. 40).
- Fried, S., Novan, K., & Peterman, W. B. (2022). Climate policy transition risk and the macroeconomy. *European Economic Review*, 147, 104174. <https://doi.org/10.1016/j.eurocorev.2022.104174> (cit. on p. 4).
- Harstad, B. (2020). Technology and Time Inconsistency. *Journal of Political Economy*, 128(7), 2653–2689. <https://doi.org/10.1086/707024> (cit. on p. 5).
- Hassett, K. A., & Metcalf, G. E. (1999). Investment with Uncertain Tax Policy: Does Random Tax Policy Discourage Investment? *The Economic Journal*, 109(457), 372–393. Retrieved November 27, 2023, from <https://www.jstor.org/stable/2565710> (cit. on p. 3).
- IEA. (2024, August). *Greenhouse Gas Emissions from Energy Highlights*. IEA. Retrieved October 24, 2025, from <https://www.iea.org/data-and-statistics/data-product/greenhouse-gas-emissions-from-energy-highlights> (cit. on p. 40).

- IEA. (2025, October 6). *Energy Statistics Data Browser – Data Tools*. IEA. Retrieved October 24, 2025, from <https://www.iea.org/data-and-statistics/data-tools/energy-statistics-data-browser?country=WORLD&fuel=Electricity%20and%20heat&indicator=TotElecCons> (cit. on p. 40).
- International Energy Agency. (2024). *World Energy Outlook 2024*. International Energy Agency. Paris. <https://www.iea.org/reports/world-energy-outlook-2024> (cit. on p. 15).
- IPCC. (2021). *Climate Change 2021 – The Physical Science Basis: Working Group I Contribution to the Sixth Assessment Report of the Intergovernmental Panel on Climate Change* (1st ed.). Cambridge University Press. <https://doi.org/10.1017/9781009157896> (cit. on p. 18).
- IPCC (Ed.). (2023). *Climate Change 2022 - Mitigation of Climate Change: Working Group III Contribution to the Sixth Assessment Report of the Intergovernmental Panel on Climate Change*. Cambridge University Press. <https://doi.org/10.1017/9781009157926> (cit. on pp. 2, 15).
- Joos, F., Roth, R., Fuglestvedt, J. S., Peters, G. P., Enting, I. G., Von Bloh, W., Brovkin, V., Burke, E. J., Eby, M., Edwards, N. R., Friedrich, T., Frölicher, T. L., Halloran, P. R., Holden, P. B., Jones, C., Kleinen, T., Mackenzie, F. T., Matsumoto, K., Meinshausen, M., ... Weaver, A. J. (2013). Carbon dioxide and climate impulse response functions for the computation of greenhouse gas metrics: A multi-model analysis. *Atmospheric Chemistry and Physics*, 13(5), 2793–2825. <https://doi.org/10.5194/acp-13-2793-2013> (cit. on pp. 37, 39, 40).
- Kalk, A., & Sorger, G. (2023). Climate policy under political pressure. *Journal of Environmental Economics and Management*, 122, 102900. <https://doi.org/10.1016/j.jeem.2023.102900> (cit. on p. 5).
- Lan, X., & Keeling, R. (2025, May 9). *Trends in Atmospheric Carbon Dioxide*. <https://gml.noaa.gov/ccgg/trends/data.html>. Retrieved October 24, 2025, from <https://gml.noaa.gov/ccgg/trends/data.html> (cit. on p. 40).
- Meinshausen, M., Raper, S. C. B., & Wigley, T. M. L. (2011). Emulating coupled atmosphere-ocean and carbon cycle models with a simpler model, MAGICC6 – Part 1: Model description and calibration. *Atmospheric Chemistry and Physics*, 11(4), 1417–1456. <https://doi.org/10.5194/acp-11-1417-2011> (cit. on p. 11).
- Pindyck, R. S. (1991). Irreversibility, Uncertainty, and Investment. *Journal of Economic Literature*, 29(3), 1110–1148. Retrieved November 16, 2023, from <https://www.jstor.org/stable/2727613> (cit. on p. 3).
- Richters, O., Kriegler, E., Bertram, C., Cui, R., Edmonds, J., Fawcett, A., Fuhrman, J., George, M., Hackstock, P., Hurst, I., Ju, Y., Kotz, M., Liadze, I., Min, J., Piontek, F., Sanchez Juanino, P., Sferra, F., Stevanovic, M., van Ruijven, B.,

- ... Zhao, X. (2024, November 5). *NGFS Climate Scenarios Data Set*. Zenodo. <https://doi.org/10.5281/zenodo.13989530> (cit. on p. 10).
- Rozenberg, J., Vogt-Schilb, A., & Hallegatte, S. (2020). Instrument choice and stranded assets in the transition to clean capital. *Journal of Environmental Economics and Management*, 100, 102183. <https://doi.org/10.1016/j.jeem.2018.10.005> (cit. on p. 3).
- Shouse, K. C., Ramseur, J. L., & Tsang, L. (2020, October 15). *EPA's Affordable Clean Energy Rule: In Brief*. (Cit. on p. 2).
- U.S. EPA. (2015, October 23). Carbon Pollution Emission Guidelines for Existing Stationary Sources: Electric Utility Generating Units. Retrieved October 25, 2025, from <https://www.govinfo.gov/content/pkg/FR-2015-10-23/pdf/2015-22842.pdf> (cit. on p. 2).
- Wright, T. P. (1936). Factors Affecting the Cost of Airplanes. *Journal of the Aero-nautical Sciences*, 3(4), 122–128. <https://doi.org/10.2514/8.155> (cit. on p. 8).

A Optimal Utilization Rates

The derivative of the electricity price with respect to electricity supply is given by

$$\frac{\partial q_t}{\partial Z} = -\frac{\beta}{Z}.$$

For $\gamma < 1$, the marginal products of green and brown capital are

$$\begin{aligned} F_G &= A^Z (\xi (\eta_G G)^\gamma + (1 - \xi)(\eta_B B)^\gamma)^{\frac{1}{\gamma}-1} \xi (\eta_G G)^{\gamma-1} \\ &= F(\eta_G G, \eta_B B)/F(\eta_G G, \eta_B B)^\gamma (A^Z)^\gamma \xi (\eta_G G)^{\gamma-1} \\ &= F(\eta_G G, \eta_B B)^{1-\gamma} (A^Z)^\gamma \xi (\eta_G G)^{\gamma-1} \end{aligned}$$

and

$$\begin{aligned} F_B &= A^Z (\xi (\eta_G G)^\gamma + (1 - \xi)(\eta_B B)^\gamma)^{\frac{1}{\gamma}-1} (1 - \xi)(\eta_B B)^{\gamma-1} \\ &= F(\eta_G G, \eta_B B)^{1-\gamma} (A^Z)^\gamma (1 - \xi)(\eta_B B)^{\gamma-1}. \end{aligned}$$

Putting this together and assuming an interior solution I find

$$\begin{aligned} -\beta F_G(\eta_G G, \eta_B B) + (\alpha - \beta \log(F(\eta_G G, \eta_B B))) F_G(\eta_G G, \eta_B B) &= 0 \\ -\beta + (\alpha - \beta \log(F(\eta_G G, \eta_B B))) &= 0 \\ F(\eta_G G, \eta_B B) &= \exp\left(\frac{\alpha}{\beta} - 1\right). \end{aligned} \quad (20)$$

$$\begin{aligned} -\beta F_B(\eta_G G, \eta_B B) + (\alpha - \beta \log(F(\eta_G G, \eta_B B))) F_B(\eta_G G, \eta_B B) &= \psi(P, m)\phi \\ (\alpha - \beta(1 + \log(F(\eta_G G, \eta_B B)))) F_B(\eta_G G, \eta_B B) &= \psi(P, m)\phi. \end{aligned} \quad (21)$$

Let us first consider the case where $m = 0$, i.e., there is no carbon tax. Then the two first-order conditions are identical and the system of equations is underdetermined. The solution set is the level curve $F = Z^*$, where $Z^* = \exp\left(\frac{\alpha_t}{\beta} - 1\right)$ is the revenue-maximizing production level. If $F(G, B) < Z^*$, all capital is used. If $F(G, B) > Z^*$, I assume a tie-breaking rule that selects the utilization rate pair with the least amount of brown energy use.

If a carbon tax is implemented, the system has a unique solution. If $F(G, 0) > Z^*$, no brown energy will be used and $\eta_G = \frac{Z^*}{A^Z \xi^{\frac{1}{\gamma}} G}$. Otherwise, green energy will be fully utilized, and η_B solves Equation 21 with $\eta_G = 1$.

B Numerical Implementation

I discretize the continuous state variables G , B , and P on an $N = N_G \times N_B \times N_P$ grid.

Let us first consider the stationary problem, where the value function does not depend on time. The HJB equations are then given by

$$\begin{aligned} \rho V(G, B, P, m) &= \max_{I^G \geq 0, I^B \geq 0, \eta \in [0, 1]^2} \left\{ q(F(\eta_G G, \eta_B B)) F(\eta_G G, \eta_B B) \right. \\ &\quad - \left(p^G(G) + \frac{\kappa_G}{2} \frac{I^G}{G} \right) I^G - \left(p^B + \frac{\kappa_B}{2} \frac{I^B}{B} \right) I^B - \psi(P, m)\phi \eta_B B \\ &\quad \left. + V_G \dot{G} + V_B \dot{B} + \lambda (V(G, B, P, -m) - V(G, B, P, m)) \right\}, \end{aligned} \quad (22)$$

The state (G, B, P, m) is a 4-dimensional vector, indexed with some abuse of notation by i, j, k, m . I approximate the derivatives using both upwind and downwind differences:

$$V_G(G_i, B_j, P_k, m) \approx \frac{V(G_{i+1}, B_j, P_k, m) - V(G_i, B_j, P_k, m)}{\Delta G} = V_{G,i,j,k,m,f} \quad (23)$$

$$V_G(G_i, B_j, P_k, m) \approx \frac{V(G_i, B_j, P_k, m) - V(G_{i-1}, B_j, P_k, m)}{\Delta G} = V_{G,i,j,k,m,b}, \quad (24)$$

where $V_{G,i,j,k,m,f}$ and $V_{G,i,j,k,m,b}$ are the upwind and downwind differences, respectively. The derivative with respect to B is defined similarly.

If V^n is the current guess of the value function, the next guess V^{n+1} is implicitly given by

$$\begin{aligned} \frac{V_{i,j,k,m}^{n+1} - V_{i,j,k,m}^n}{\Delta} + \rho V_{i,j,k,m}^{n+1} &= q(\eta_{G,i,j,k,m}, \eta_{B,i,j,k,m} B_j) F(\eta_{G,i,j,k,m} G_i, \eta_{B,i,j,k,m} B_j) \\ &\quad - \left(p_{i,j,k,m}^G + \frac{\kappa_G}{2} \frac{I_{G,i,j,k,m}^n}{G_i} \right) I_{G,i,j,k,m}^n \\ &\quad - \left(p^B + \frac{\kappa_B}{2} \frac{I_{B,i,j,k,m}^n}{B_j} \right) I_{B,i,j,k,m}^n \\ &\quad - \psi(P_k, m) \phi \eta_{B,i,j,k,m} B_j \\ &\quad + (V_{G,i,j,k,m}^{n+1})' (I_{G,i,j,k,m}^n - \delta_G G_i) \\ &\quad + (V_{B,i,j,k,m}^{n+1})' (I_{B,i,j,k,m}^n - \delta_B B_j) \\ &\quad + \lambda (V_{i,j,k,-m}^{n+1} - V_{i,j,k,m}^{n+1}), \end{aligned} \quad (25)$$

where $I_{G,i,j,k,m}^n$ and $I_{B,i,j,k,m}^n$ are the optimal investments based on the n -th iteration of the value function. This is a semi-implicit scheme, as the optimal policies are calculated with the n -th iteration of the value function. The term $\frac{V_{i,j,k,m}^{n+1} - V_{i,j,k,m}^n}{\Delta}$ is a fictitious time derivative that is close to zero if the value function has converged.

The optimal brown capital utilization rate is independent of the value function and can therefore be calculated a priori.

Let the drift of capital $K \in \mathcal{K} = \{G, B\}$ be given by

$$\mu_{K,i,j,k,m,f}^n = \max \left(0, \frac{1}{\kappa_K} (V_{K,i,j,k,f}^n - p_{i,j,k,m}^K) \right) - \delta_K K_i \quad (26)$$

$$\mu_{K,i,j,k,m,b}^n = \max \left(0, \frac{1}{\kappa_K} (V_{K,i,j,k,b}^n - p_{i,j,k,m}^K) \right) - \delta_K K_i. \quad (27)$$

The upwind scheme uses V'_f when $\mu_f^n > 0$ and V'_b when $\mu_b^n < 0$. When $\mu_f^n < 0$ and $\mu_b^n > 0$, I set net capital accumulation to zero, which implies investment exactly offsets the depreciation, i.e.

$$\bar{V}'_{K,i,j,k,m} = p_{i,j,k,m}^K + \kappa_K \delta_K K_i. \quad (28)$$

In case the forward drift is positive and the backward drift is negative, I use the value of the Hamiltonian calculated using the forward- and backward-differences as a tiebreaker as noted in Achdou et al. (2022). The Hamiltonian is calculated separately for each capital stock assuming the investment in the other capital stock is of the magnitude to keep it at the same level. The choice of the investment in the other capital stock is not important as long as they are the same in both cases. The Hamiltonians for G are given by

$$\begin{aligned} \mathcal{H}_{G,i,j,k,m,f}^n &= q(\eta_{G,i,j,k,m} G_i, \eta_{B,i,j,k,m} B_j) F(\eta_{G,i,j,k,m} G_i, \eta_{B,i,j,k,m} B_j) \\ &\quad - \left(p_{i,j,k,m}^G + \frac{\kappa_G}{2} \frac{I_{G,i,j,k,m,f}^n}{G_i} \right) I_{G,i,j,k,m,f}^n - \left(p^B + \frac{\kappa_B}{2} \frac{\bar{I}_{B,i,j,k,m}^n}{B_j} \right) \bar{I}_{B,i,j,k,m}^n \\ &\quad - \psi(P_k, m) \phi \eta_{B,i,j,k,m} B_j + \frac{V_{i+1,j,k,m}^n - V_{i,j,k,m}^n}{\Delta G} (\mu_{G,i,j,k,m,f}^n), \end{aligned} \quad (29)$$

$$\begin{aligned} \mathcal{H}_{G,i,j,k,m,b}^n &= q(\eta_{G,i,j,k,m} G_i, \eta_{B,i,j,k,m} B_j) F(\eta_{G,i,j,k,m} G_i, \eta_{B,i,j,k,m} B_j) \\ &\quad - \left(p_{i,j,k,m}^G + \frac{\kappa_G}{2} \frac{I_{G,i,j,k,m,b}^n}{G_i} \right) I_{G,i,j,k,m,b}^n - \left(p^B + \frac{\kappa_B}{2} \frac{\bar{I}_{B,i,j,k,m}^n}{B_j} \right) \bar{I}_{B,i,j,k,m}^n \\ &\quad - \psi(P_k, m) \phi \eta_{B,i,j,k,m} B_j + \frac{V_{i,j,k,m}^n - V_{i-1,j,k,m}^n}{\Delta G} (\mu_{G,i,j,k,m,b}^n), \end{aligned} \quad (30)$$

with the Hamiltonians for B defined similarly.

If the gain in the forward direction is higher than in the backward direction, I use the forward difference, otherwise I use the backward difference.

Putting this in a single equation,

$$V_{K,i,j,k,m}^{n'} = \begin{cases} V_{K,i,j,k,m,f}^n & \text{if } (\mu_{K,i,j,k,m,f}^n > 0 \wedge \mu_{K,i,j,k,m,b}^n \geq 0) \vee \\ & ((\mu_{K,i,j,k,m,f}^n > 0 \wedge \mu_{K,i,j,k,m,b}^n < 0) \wedge \mathcal{H}_{K,i,j,k,m,f}^n > \mathcal{H}_{K,i,j,k,m,b}^n) \\ V_{K,i,j,k,m,b}^n & \text{if } (\mu_{K,i,j,k,m,f}^n \leq 0 \wedge \mu_{K,i,j,k,m,b}^n < 0) \vee \\ & ((\mu_{K,i,j,k,m,f}^n > 0 \wedge \mu_{K,i,j,k,m,b}^n < 0) \wedge \mathcal{H}_{K,i,j,k,m,f}^n < \mathcal{H}_{K,i,j,k,m,b}^n) \\ \bar{V}_{K,i,j,k,m}^n & \text{if } (\mu_{K,i,j,k,m,f}^n < 0 \wedge \mu_{K,i,j,k,m,b}^n > 0) \end{cases}$$

where $K \in \{G, B\}$.

Let,

$$\begin{aligned}\pi_{i,j,k,m}^n &= q(\eta_{G,i,j,k,m} G_i, \eta_{B,i,j,k,m} B_j) F(\eta_{G,i,j,k,m} G_i, \eta_{B,i,j,k,m} B_j) \\ &\quad - \left(p_{i,j,k,m}^G + \frac{\kappa_G}{2} \frac{I_{G,i,j,k,m}^n}{G_i} \right) I_{G,i,j,k,m}^n - \left(p^B + \frac{\kappa_B}{2} \frac{I_{B,i,j,k,m}^n}{B_j} \right) I_{B,i,j,k,m}^n \\ &\quad - \psi(P_k, m) \phi \eta_{B,i,j,k,m} B_j.\end{aligned}\tag{31}$$

Then,

$$\begin{aligned}\frac{V_{i,j,k,m}^{n+1} - V_{i,j,k,m}^n}{\Delta} + \rho V_{i,j,k,m}^{n+1} &= \pi_{i,j,k,m}^n \\ &\quad + \frac{V_{i+1,j,k,m}^{n+1} - V_{i,j,k,m}^{n+1}}{\Delta G} (\mu_{G,i,j,k,m,f}^n)^+ + \frac{V_{i,j,k,m}^{n+1} - V_{i-1,j,k,m}^{n+1}}{\Delta G} (\mu_{G,i,j,k,m,b}^n)^- \\ &\quad + \frac{V_{i,j+1,k,m}^{n+1} - V_{i,j,k,m}^{n+1}}{\Delta B} (\mu_{B,i,j,k,m,f}^n)^+ + \frac{V_{i,j,k,m}^{n+1} - V_{i,j-1,k,m}^{n+1}}{\Delta B} (\mu_{B,i,j,k,m,b}^n)^- \\ &\quad + \lambda (V_{i,j,k,-m}^{n+1} - V_{i,j,k,m}^{n+1}).\end{aligned}\tag{32}$$

Collecting terms with the same subscripts, yields

$$\begin{aligned}\frac{V_{i,j,k,m}^{n+1} - V_{i,j,k,m}^n}{\Delta} + (\rho + \lambda) V_{i,j,k,m}^{n+1} &= \pi_{i,j,k,m}^n \\ &\quad + V_{i-1,j,k,m}^{n+1} x_{G,i,j,k,m} + V_{i,j,k,m}^{n+1} y_{G,i,j,k,m} + V_{i+1,j,k,m}^{n+1} z_{G,i,j,k,m} \\ &\quad + V_{i,j-1,k,m}^{n+1} x_{B,i,j,k,m} + V_{i,j,k,m}^{n+1} y_{B,i,j,k,m} + V_{i,j+1,k,m}^{n+1} z_{B,i,j,k,m} \\ &\quad + \lambda V_{i,j,k,-m}^{n+1},\end{aligned}\tag{33}$$

where

$$\begin{aligned}x_{K,i,j,k,m} &= -\frac{(\mu_{K,i,j,k,m,b}^n)^-}{\Delta K}, \\ y_{K,i,j,k,m} &= -\frac{(\mu_{K,i,j,k,m,f}^n)^+}{\Delta K} + \frac{(\mu_{K,i,j,k,m,b}^n)^-}{\Delta K}, \\ z_{K,i,j,k,m} &= \frac{(\mu_{K,i,j,k,m,f}^n)^+}{\Delta K}.\end{aligned}$$

For example, $x_{G,i,j,k,m}$ will denote the rate at which the state variable moves from (i, j, k, m) to $(i - 1, j, k, m)$, and $z_{G,i,j,k,m}$ will denote the rate at which the state variable moves from (i, j, k, m) to $(i + 1, j, k, m)$.

In addition, with probability λ , the state variable jumps to $-m$, so the diagonal element of the matrix is given by $\sum_{s \in \{G,B\}} y_{s,i,j,k,m} - \lambda$ and $A_{i,j,k,-m}^n = \lambda$.

Now this will yield a system of $2 \times N_G \times N_B \times N_P$ equations. This system needs to be reshaped by transforming the $2 \times N_G \times N_B \times N_P$ grid into a vector of length $2 \times N_G \times N_B \times N_P$.

Let us index this combined vector by l , where $l = 1, 2, \dots, 2 \times N_G \times N_B \times N_P$.

Then each equation (33) becomes the l -th row of a sparse linear system

$$\mathbf{M}^n \mathbf{V}^{(n+1)} = \mathbf{b}^n, \quad (34)$$

where \mathbf{M}^n is a $(2 N_G N_B N_P) \times (2 N_G N_B N_P)$ matrix, given by

$$\mathbf{M}^n = \left(\frac{1}{\Delta} + \rho + \lambda \right) I_{2 N_G N_B N_P} - \mathbf{A}^n, \quad (35)$$

and \mathbf{b}^n is a $(2 N_G N_B N_P)$ -dimensional vector, given by

$$b_l^n = \pi_{i,j,k,m}^n + \frac{1}{\Delta} V_{i,j,k,m}^n. \quad (36)$$

B.1 Nonautonomous problem

In the nonautonomous problem, some of the parameters are time-dependent. In particular, I let q depend on time.

The nonautonomous problem is given by

$$\begin{aligned} \rho V_t(G, B, P, m) &= \max_{I^G \geq 0, I^B \geq 0, \eta \in [0,1]^2} \left\{ q_t(F(\eta_G G, \eta_B B)) F(\eta_G G, \eta_B B) \right. \\ &\quad - \left(p^G(G) + \frac{\kappa_G}{2} \frac{I^G}{G} \right) I^G - \left(p^B + \frac{\kappa_B}{2} \frac{I^B}{B} \right) I^B - \psi(P, m) \phi \eta_B B \\ &\quad \left. + V_{t,G} \dot{G} + V_{t,B} \dot{B} + \dot{V}_t + \lambda (V_t(G, B, P, -m) - V_t(G, B, P, m)) \right\}. \end{aligned} \quad (37)$$

In order to solve this problem, I assume that far in the future the time-dependent parameters reach a steady state, such that the nonautonomous problem becomes

autonomous and I can solve for this autonomous value function using the method described above. Here I take this time to be $\bar{t} = 2420$, which is the final period in DICE2023 (Barrage & Nordhaus, 2024). This implies that I assume that there is no more exogenous technological progress and population growth after 2420 that may cause energy demand to change. In case this seems like a strong assumption to you, as long as the time horizon is sufficiently long relative to the discount rate, the effect of what is assumed to happen after the end of the time horizon is negligible.

Let us denote the final time value function by $V^\infty(G, B, P, m)$.

For $n = \bar{t} - 1$

$$(\rho + \lambda) V^n = \pi^\infty + \mathbf{A}^\infty V^n + \frac{1}{\Delta} (V^\infty - V^n), \quad (38)$$

where V^∞ is the value function at the steady state.

Then, the nonautonomous problem can be solved backwards in time

$$(\rho + \lambda) V^n = \pi^{n+1} + \mathbf{A}^{n+1} V^n + \frac{1}{\Delta} (V^{n+1} - V^n). \quad (39)$$

So that V^n is given by the solution to

$$\left(\left(\frac{1}{\Delta} + \rho + \lambda \right) I_{2N_G N_B N_P} - \mathbf{A}^{n+1} \right) V^n = \pi^{n+1} + \frac{1}{\Delta} V^{n+1}. \quad (40)$$

Note that the optimal choices are calculated based on the previous value function. Also note that even though the sign of the time derivative in the HJB is different from the autonomous case, the actual updating of the value function is the same, except that previously index was marched forward in index n – which in the autonomous case is unrelated to calendar time – and now it is marched backwards in n until the initial time period t_0 is reached.

C Calibration

I calibrate the model to the world economy in 2012. Some of the parameters are taken from Baldwin et al. (2020) and sources therein.

The decay rate of carbon in the atmosphere ϑ is calibrated based on Joos et al. (2013), which is also the basis of the AR6 (“The Earth’s Energy Budget, Climate Feedbacks and Climate Sensitivity”, 2023). They simulate impulse response functions of carbon

Variable	Units	Description
G	TW	Green energy capacity ¹
B	TW	Brown energy capacity
Z	PWh	Total energy production in a year
E	Gt CO ₂ yr ⁻¹	annual carbon emissions from electricity generation
θ		share of green energy in total energy production
A^Z		Total energy productivity multiplier
q	T2010\$/PWh	price of energy
κ_G	T2010\$ TW ⁻¹ yr	green investment adjustment cost multiplier
κ_B	T2010\$ TW ⁻¹ yr	brown investment adjustment cost multiplier
p^G	T2010\$/TW	price of green energy capital
p^B	T2010\$/TW	price of brown energy capital
δ	yr ⁻¹	depreciation rate of energy capital
ϕ	Gt CO ₂ yr ⁻¹ TW ⁻¹	carbon emissions per unit of energy capacity used
γ		1 – 1/elasticity of substitution

¹ Excluding hydropower as in Baldwin et al. (2020) due to it being already a matured form of electricity generation with little learning potential and many of the suitable sites already being used, so further expansion is difficult.

Table 1: Energy variables and parameters

Variable	Units	Description
p_0^G	T2010\$	initial investment price of green capital
G_0	TW	initial level of green capital
b		Progress rate parameter

Table 2: Learning-by-doing parameters

Variable	Units	Description
λ		Hazard rate of tax regime
τ_0	T2010\$/GtCO ₂	tax function parameter
τ_1		tax function parameter

Table 3: Government

Variable	Units	Description
P	Gt CO ₂	stock of atmospheric CO ₂ in gigatonnes
ϑ	yr ⁻¹	pollution decay rate

Table 4: Climate variables

in the atmosphere as a response to a pulse emission of 100 GtC aggregating multiple carbon cycle models. Their impulse response functions has more time scales, allowing for a more accurate representation of the carbon cycle. In this paper, there is only one decay rate, which I calibrate to match the e-folding time of their aggregate impulse response function 100 years after the pulse emission. The e-folding time is the time it takes for the initial pulse to decay to $1/e \approx 36.8\%$ of its initial value. I choose ϑ such that the fraction of carbon remaining in the atmosphere after 100 years is the same in both models. This gives an e-folding time of approximately 112 years, i.e., $\vartheta = 1/112\text{yr}^{-1}$. This specification is fairly accurate for the first 100 years after the pulse emission, but underestimates the long-term carbon remaining in the atmosphere compared to Joos et al. (2013).

D Robustness

D.1 Higher tax levels

In the main text, I present results for two tax schedules — *Current Policies* and *NDCs* — that represent plausible near-term paths. To test robustness, I consider a third schedule, *Below 2°C*, which based on the integrated assessment models (IAM) used by the NGFS manages to keep warming below 2 °C with high probability.

The state variable paths under *Below 2°C* with an expected duration of 8 years are shown in Figure 15. The dynamics are qualitatively similar compared to *NDCs*.

Variable	Value	Source
t_0	2012	Baldwin et al. (2020)
G_0	0.46 TW	Baldwin et al. (2020)
B_0	3.61 TW	Baldwin et al. (2020)
Z_0	18.94 PW h yr ⁻¹	IEA (2025) Final Energy Consumption
p_0^G	2.11 T2010\$/TW	Baldwin et al. (2020)
p^B	0.57 T2010\$/TW	Baldwin et al. (2020)
q_0	0.0984 T2010\$/PWh	EIA (2023) Average U.S. retail electricity price
P_0	3075 Gt CO ₂	Lan and Keeling (2025) Mean atmospheric CO ₂ concentration at Mauna Loa
E_0	13.0 Gt CO ₂ yr ⁻¹	IEA (2024) estimated CO ₂ emissions from electricity generation

Table 5: Calibrated variables

Parameter	Value	Source
ρ	0.03 yr ⁻¹	
δ_G	0.025 yr ⁻¹	
δ_B	0.025 yr ⁻¹	Baldwin et al. (2020)
κ_G	0.5 T2010\$ TW ⁻¹ yr	
κ_B	0.5 T2010\$ TW ⁻¹ yr	
ϕ	3.65 Gt CO ₂ yr ⁻¹ TW ⁻¹	calibrated to match E_0 assuming full brown capital utilization
b	0.32	
γ	0.8	
ξ	0.5	
ϑ	$\frac{1}{112}$ yr ⁻¹	based on Joos et al. (2013)

Table 6: Calibrated parameters

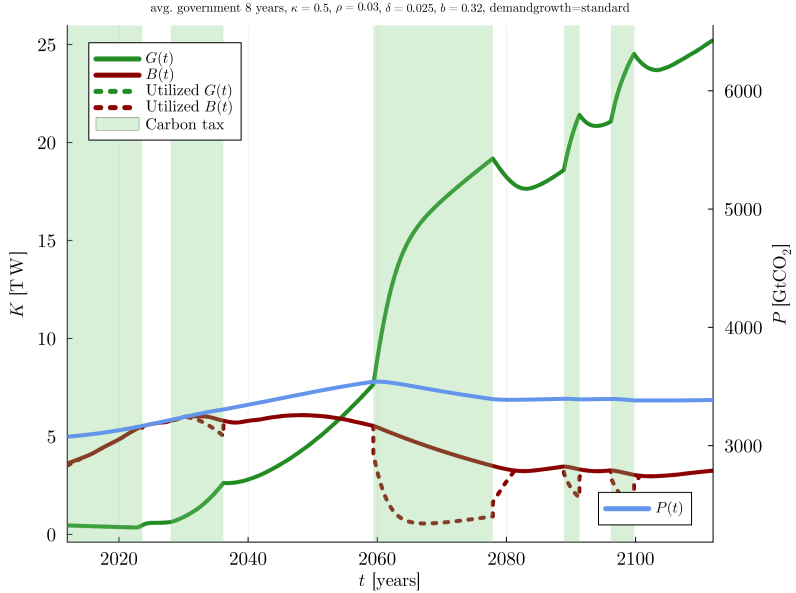


Figure 15: Evolution of state variables under the *Below 2°C* tax schedule with an expected regime duration of 8 years.

(Figure 6) but green capacity builds up earlier and brown capacity is underutilized more strongly.

The patterns for brown capacity (Figure 16), green capacity (Figure 17), and pollution (Figure 18) are also similar to those under *NDCs* (Figures 7, 8, and 9). Median paths are close across expected durations, while forecast intervals widen with longer expected durations. Overall, the results under *Below 2°C* confirm the main findings in the paper.

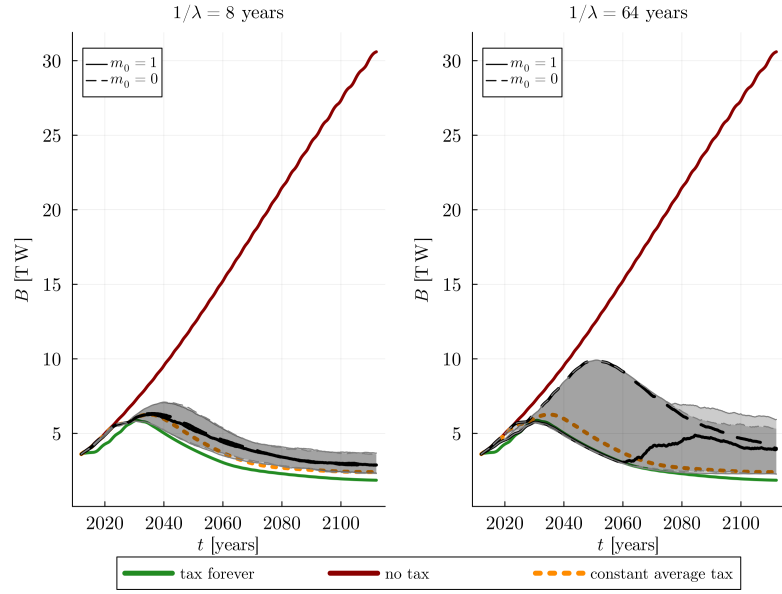


Figure 16: Brown energy capacity under the *Below 2°C* tax schedule for different expected regime durations.

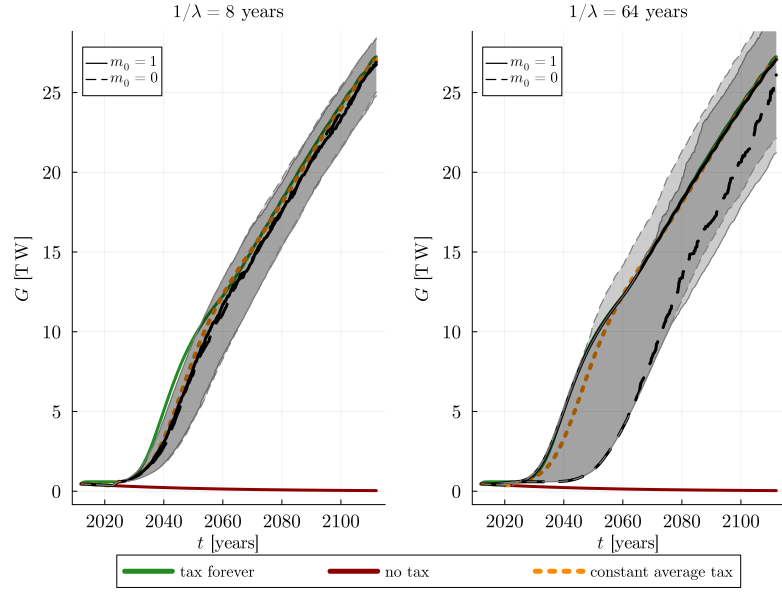


Figure 17: Green energy capacity under the *Below 2°C* tax schedule for different expected regime durations.

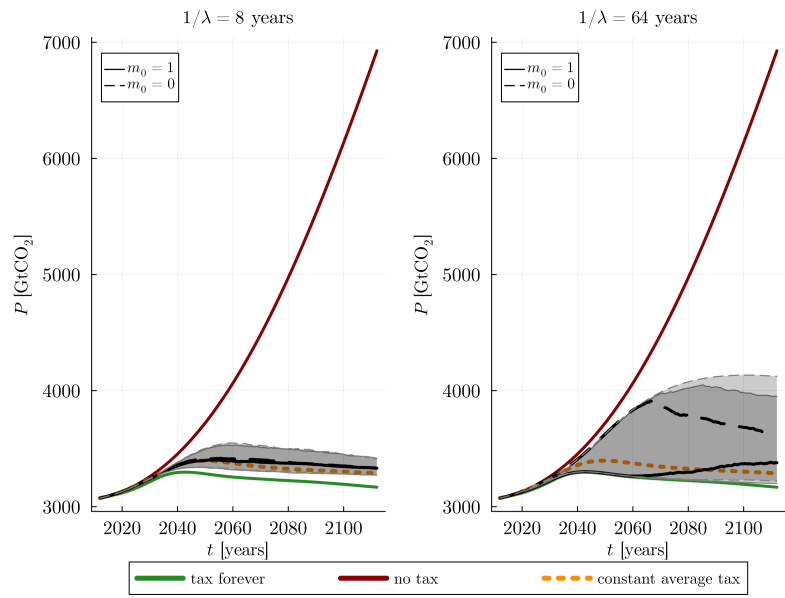


Figure 18: Pollution under the *Below 2°C* tax schedule for different expected regime durations.